Supplementary Information for

Cooperativity between the Orthosteric and Allosteric Ligand Binding Sites of RORγt

Rens M.J.M. de Vries,[§,†] Femke A. Meijer,[§,†] Richard G. Doveston,[†,‡] Iris A. Leijten-van de Gevel[†] and Luc Brunsveld[†,*]

[§] These authors contributed equally to this work.

[†] Laboratory of Chemical Biology, Department of Biomedical Engineering and Institute for Complex Molecular Systems, Technische Universiteit Eindhoven, Den Dolech 2, 5612 AZ Eindhoven, The Netherlands.

[‡] Leicester Institute of Structural and Chemical Biology and Department of Chemistry, University of Leicester, University Road, Leicester, UK, LE1 7RH.

* Luc Brunsveld
Address: P.O. Box 513 (Helix STO 3.37), 5600 MB Eindhoven, The Netherlands
Phone number: +3140 247 2870/5378
Email: l.brunsveld@tue.nl

This PDF file includes:

>   Figures S1 to S26
>   Tables S1 to S7
>   Legends for Movies S1

Other supplementary materials for this manuscript include the following:
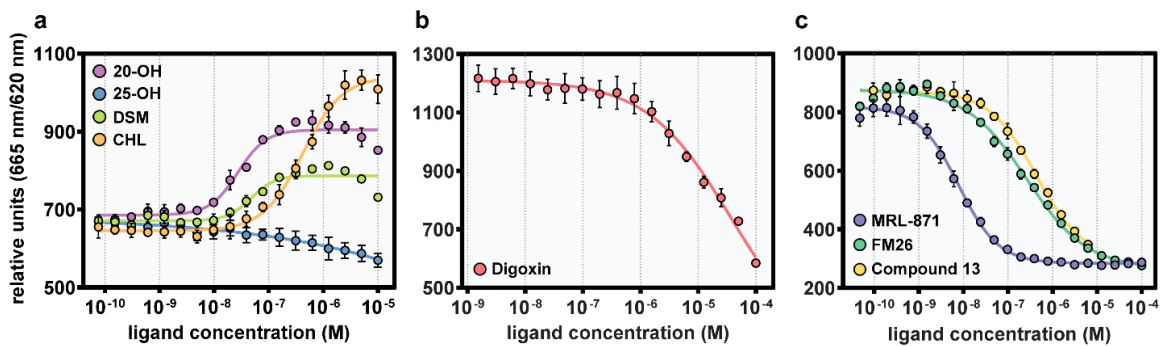
>   Movies S1

Fig. S1. Dose-response curves from the TR-FRET coactivator assay: titration of all ligands used in the manuscript to a fixed concentration of the RORγt LBD (20 nM). a Cholesterol, desmosterol, 20α-hydroxycholesterol and 25-hydroxycholesterol (orthosteric agonists). b Digoxin (orthosteric inverse agonist). c MRL-871, FM26 and compound 13 (allosteric inverse agonists). Data recorded in triplicate from three independent experiments (one representative dataset shown). Error bars represent the SD of the mean.
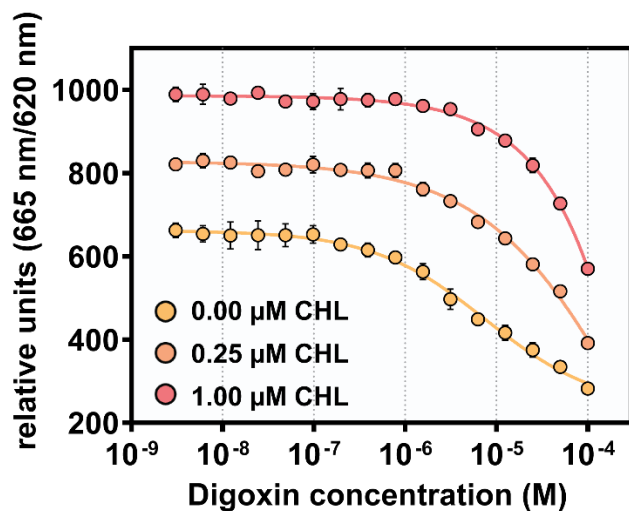
Fig. S2. Dose-response curves from the competitive TR-FRET coactivator recruitment assay with fixed concentrations of cholesterol (0.00 µM, 0.25 µM and 1.00 µM) and titration of digoxin. Data recorded in triplicate from three independent experiments (one representative dataset shown). Error bars represent the SD of the mean.
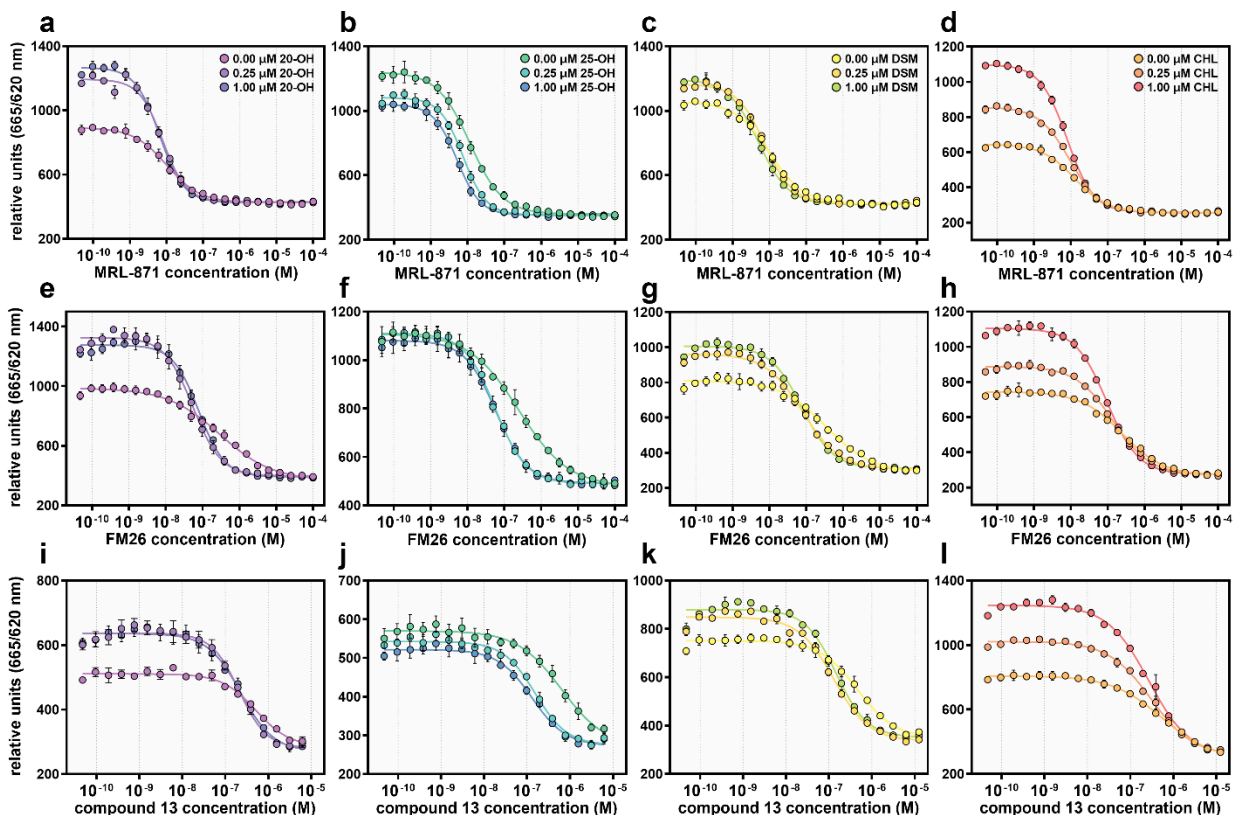
Fig. S3. Non-normalized data of the data shown in Figure 3a-l, Dose-response curves of competitive TR-FRET coactivator recruitment assays (a-l) by titration of allosteric ligands MRL-871 (a-d), FM26 (e-h) and compound 13 (i-l) to RORγt in the presence of fixed concentrations of 20α-hydroxycholesterol (20-OH) (a,e,i), 25-hydroxycholesterol (25-OH) (b,f,j), desmosterol (DSM) (c,g,k) and cholesterol (CHL) (d,h,j) (0.00 µM, 0.25 µM and 1.00 µM). Data recorded in triplicate from three independent experiments (one representative dataset shown). Error bars represent the SD of the mean.
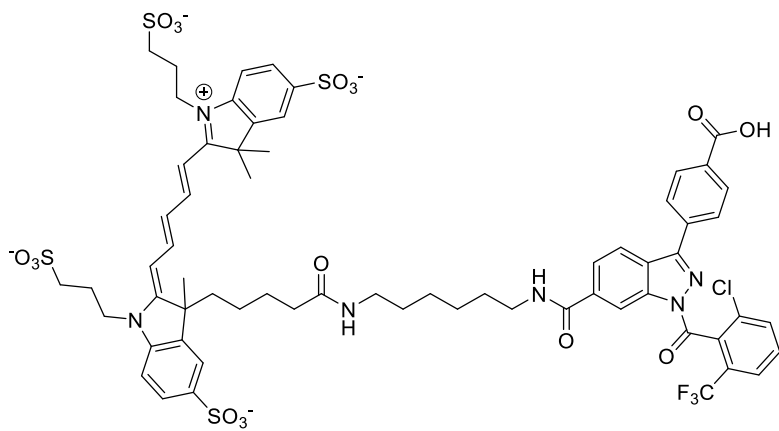
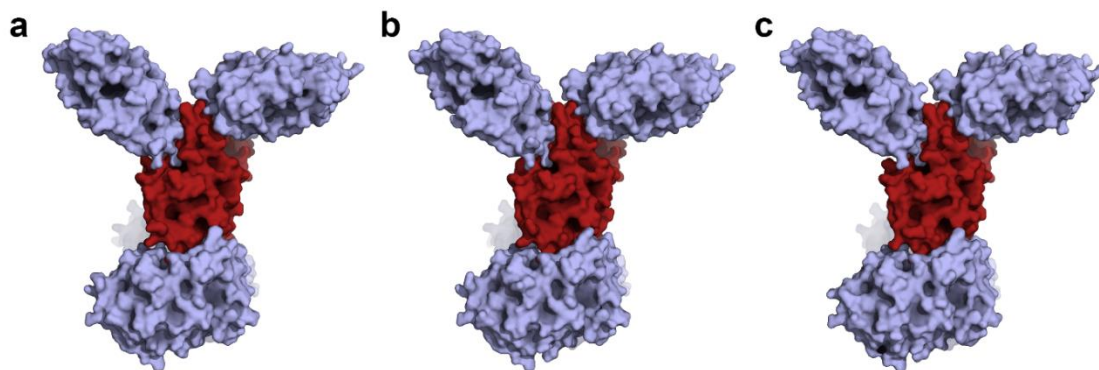**Fig. S4.** Chemical structure of AlexaFluor-MRL-871 probe.

Fig. S5. Comparison of the crystal packing of RORγt using different crystallization buffers. The RORγt monomer is shown as a red surface and directly neighboring crystallographic symmetry-mates are shown in blue. **a**, 20α-hydroxycholesterol + MRL-871 without the addition of crystallization buffer **b**, 25-hydroxycholesterol + MRL-871 in 1.6M AmSO$_4$ + 0.1M Tris (pH=8.5) **c**, desmosterol + MRL-871 in 0.2M MgCl$_2$ + 6% PEG6000 + 0.1 M Tris (pH=8.5).
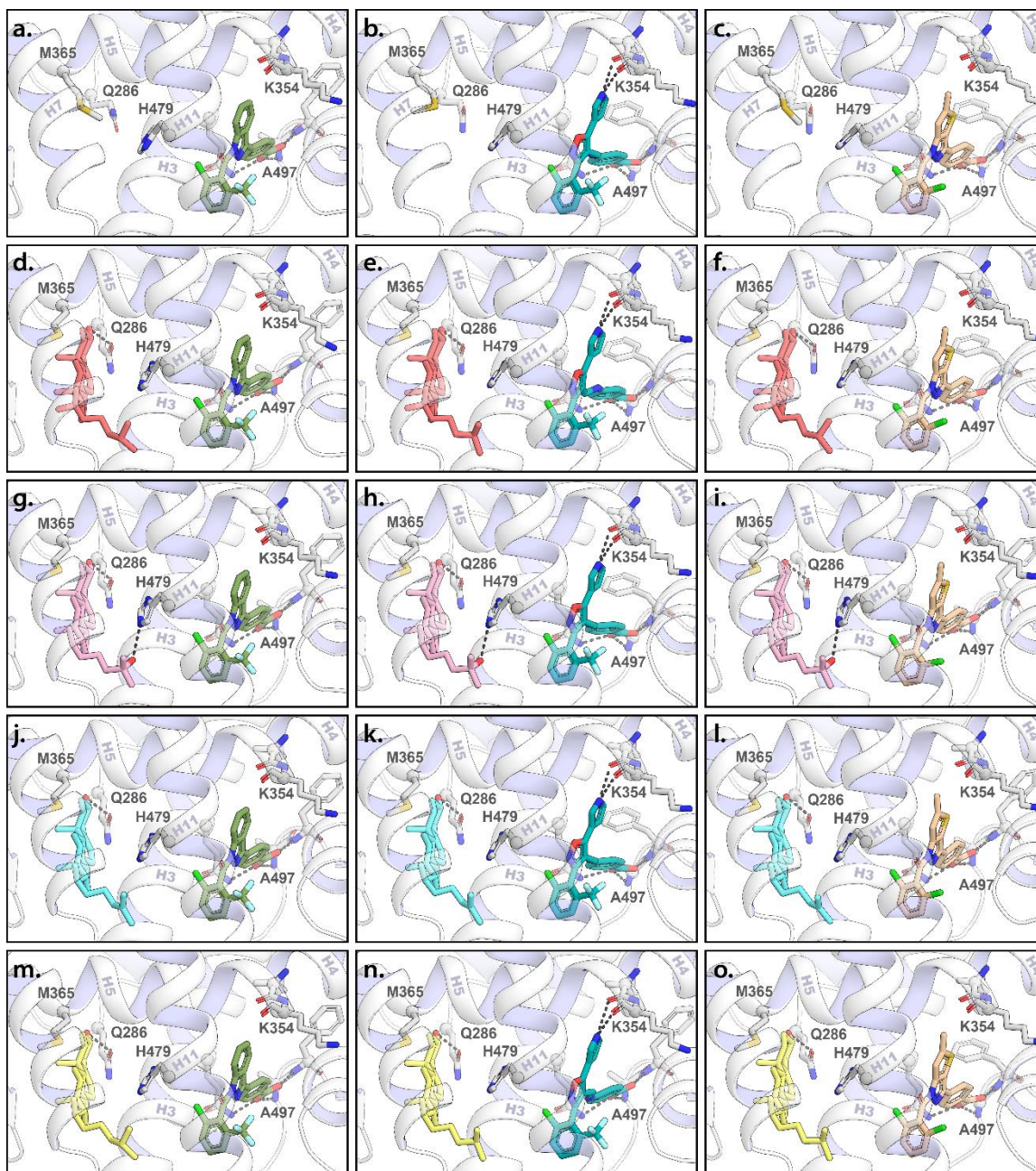
Fig S6. Crystal structures of RORγt in complex with orthosteric and allosteric ligands. a-c, Focused view of the orthosteric and allosteric ligand-binding pockets from the previously published crystal structures containing only an allosteric ligand (MRL-871 (PDB: 5C4O) in green; FM26 (PDB: 6SAL) in teal or compound 13 (PDB: 6TLM) in brown). d-o, The orthosteric and allosteric ligand-binding pocket of RORγt in the presence of 12 combinations of orthosteric and allosteric ligands (20α-hydroxycholesterol in red, 25-hydroxycholesterol in pink, desmosterol in blue and cholesterol in yellow).
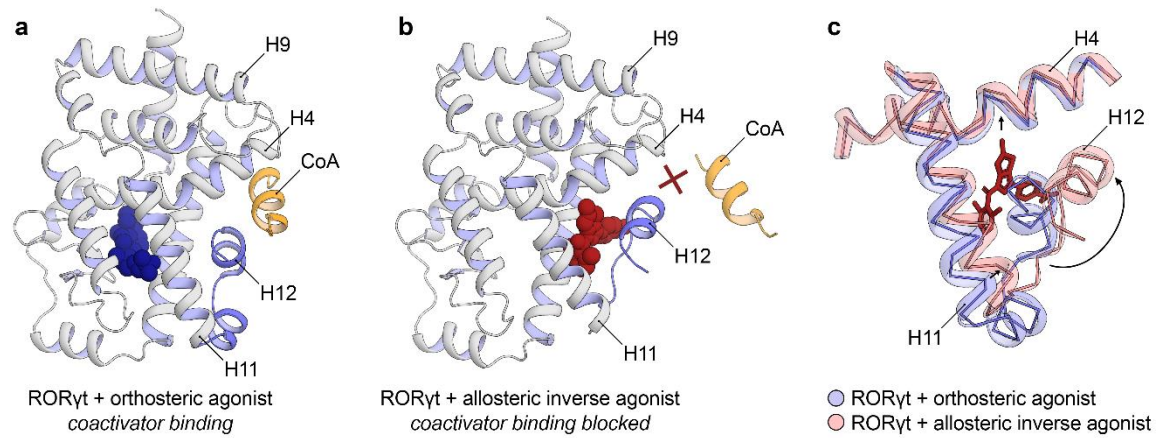
7

Fig S7. Crystal structure of RORγt in complex with **a**, an orthosteric agonist and a coactivator peptide (PDB: 3L0L) **b**, allosteric inverse agonist (PDB: 6TLM), which induces a conformation of helix 12 that prevents coactivator binding. **c**, Comparison of the allosteric ligand-binding pocket of RORγt. RORγt in complex with an orthosteric agonist and an allosteric inverse agonist are shown in blue and red, respectively. The arrows indicate the helix movement upon binding an allosteric inverse agonist.
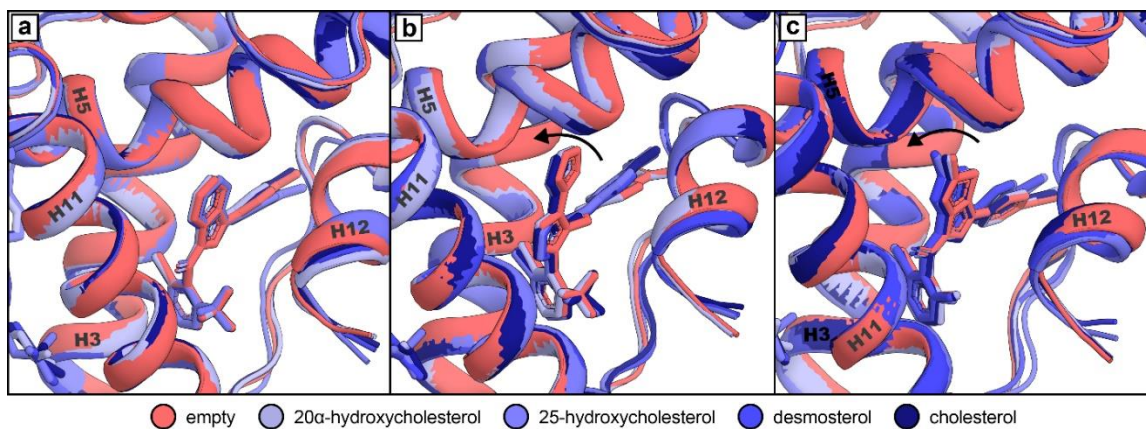
Fig. S8. Comparison of the allosteric ligand binding mode in the crystal structures in absence (red) or presence of orthosteric ligands (blue-tones). Structural overlay of crystal structures containing **a,** MRL-871 **b,** FM26 **c,** compound 13.
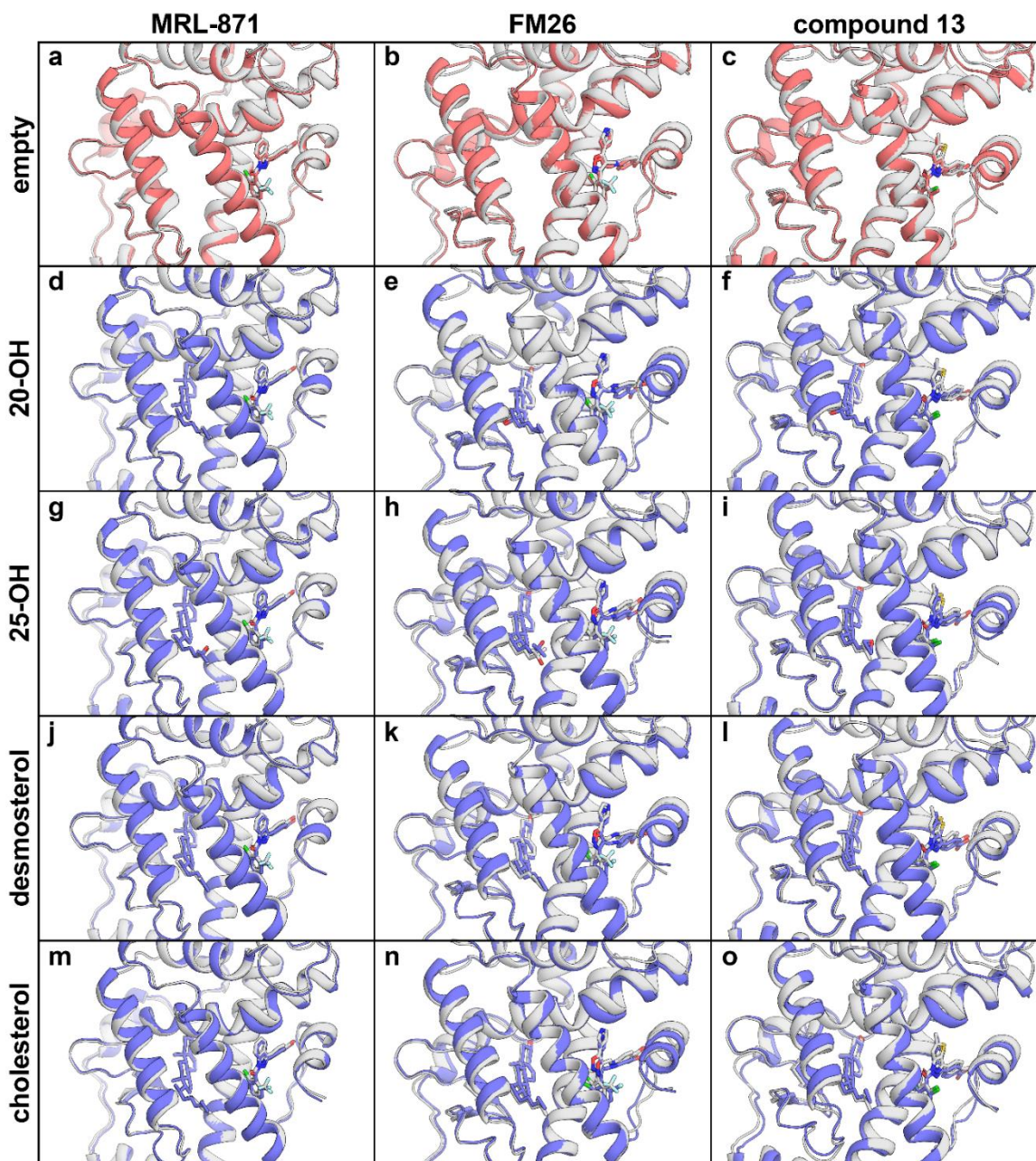
Fig. S9. Comparison of the crystal structure (white cartoon) and the average coordinates derived from the molecular dynamics simulations (red or blue cartoon). For the averaged structures, some unphysical bond lengths are present due to the averaging process.
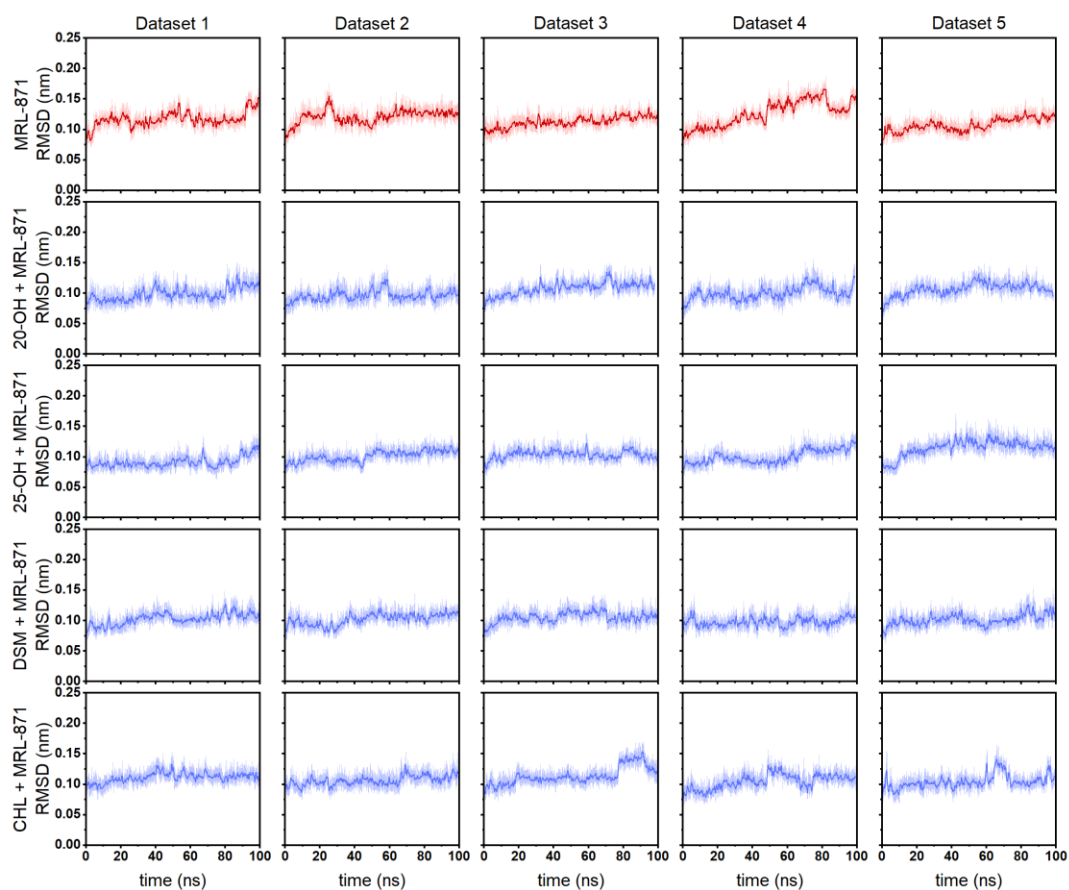
Fig. S10. Root mean square deviation (RMSD) of RORγt in complex with MRL-871 (red) and MRL-871 in presence of different orthosteric modulators (blue). Data of each dataset was plotted individually using the first frame of each simulation was used as the reference structure. The dark line was obtained using the Savitzky-Golay smoothing method using a 100-point quadratic polynomial.
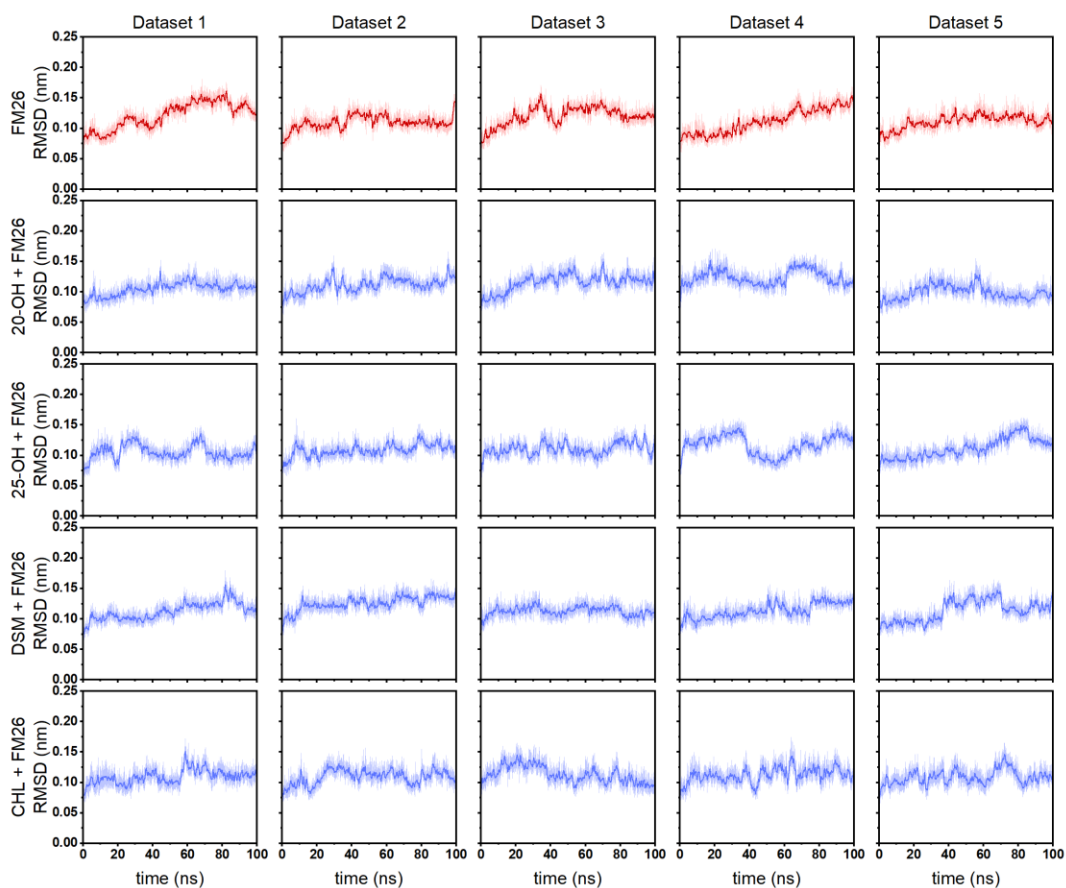
Fig. S11. Root mean square deviation (RMSD) of RORγt in complex with FM26 (red) and FM26 in presence of different orthosteric modulators (blue). Data of each dataset was plotted individually using the first frame of each simulation was used as the reference structure. The dark line was obtained using the Savitzky-Golay smoothing method using a 100-point quadratic polynomial.
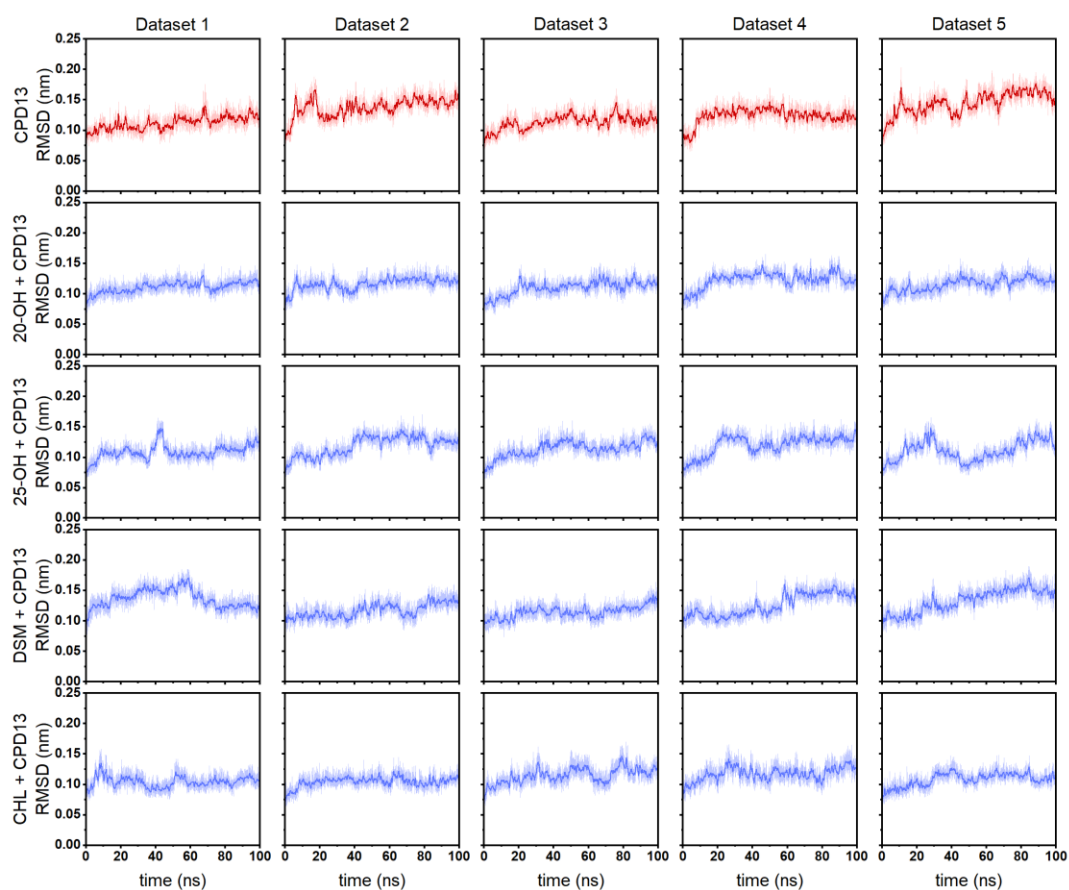
Fig. S12. Root mean square deviation (RMSD) of RORγt in complex with compound 13 (red) and compound 13 in presence of different orthosteric modulators (blue). Data of each dataset was plotted individually using the first frame of each simulation was used as the reference structure. The dark line was obtained using the Savitzky-Golay smoothing method using a 100-point quadratic polynomial.
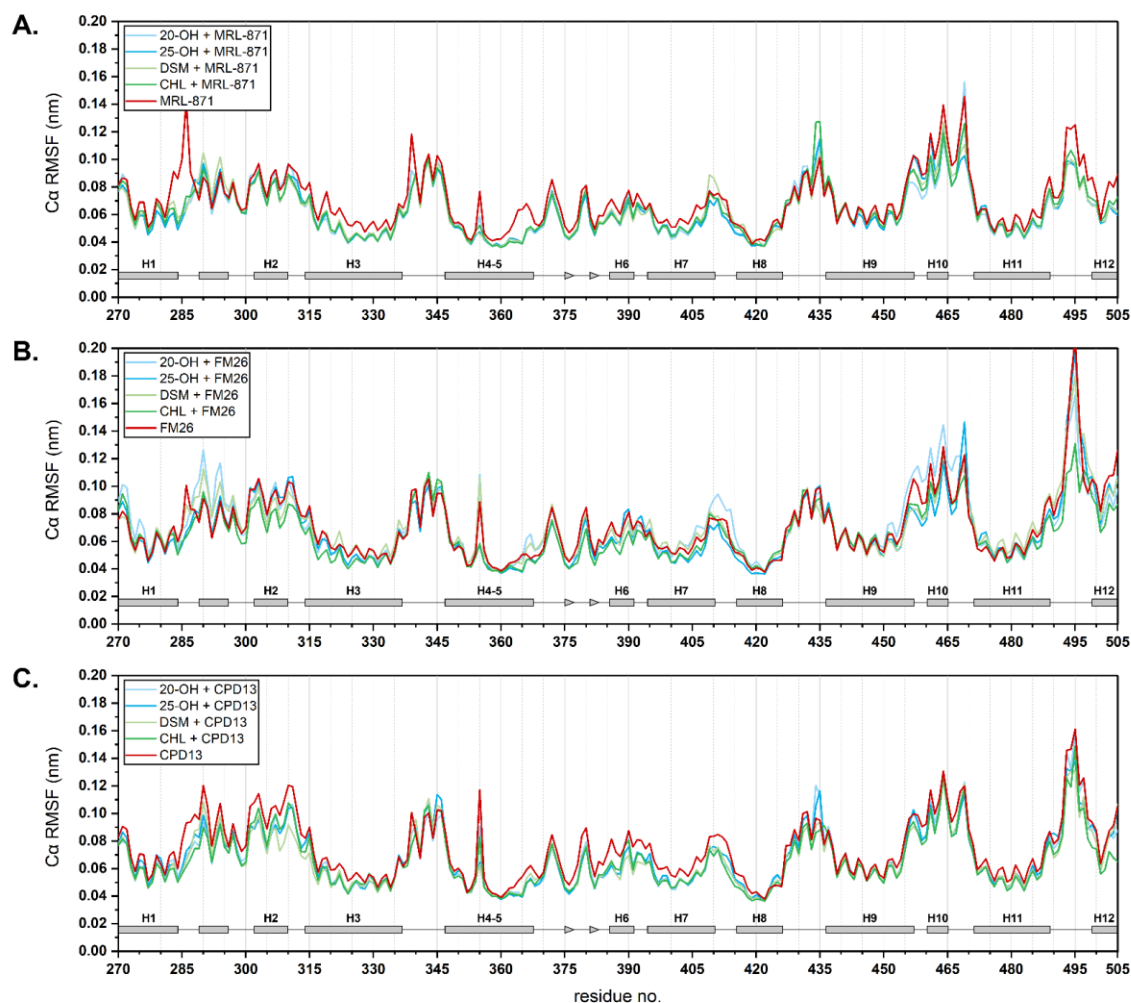
Fig. S13. a-c, Average root mean square fluctuation (RMSF) of the α-carbons of RORγt in complex with different orthosteric and allosteric ligands derived from five simulations per complex. The red lines show the RMSF in absence of an orthosteric modulator. The secondary structure of the protein is represented as a rectangle, triangle and a line for α-helices, β-sheets and loops respectively.

14
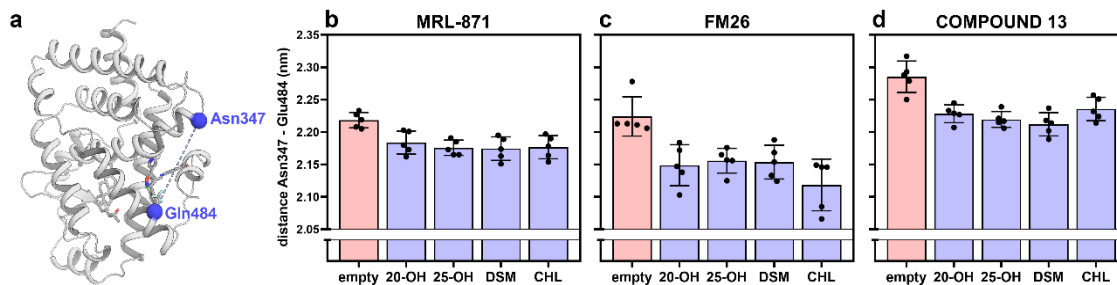
Fig. S14. Distance between the alpha carbons of Asn347 and Gln484. a, Cartoon representation of RORγt showing the positions of the alpha carbons of Asn347 and Gln484 as blue spheres. The dotted line represents the measured distance. b-d, Bars represent the average distance between the alpha carbons of Asn347 and Gln484 over five independent simulations with the individual values represented as black spheres and the error bar showing the standard deviation.

Fig. S15. Stereo image of a portion of the electron density map (2Fo-Fc) of RORγt in complex with 20α-hydroxycholesterol and MRL-871 (6T4U).

Fig. S16. Stereo image of a portion of the electron density map (2Fo-Fc) of RORγt in complex with 20α-hydroxycholesterol and FM26 (6T4T).

Fig. S17. Stereo image of a portion of the electron density map (2Fo-Fc) of RORγt in complex with 20α-hydroxycholesterol and compound 13 (6T4W).
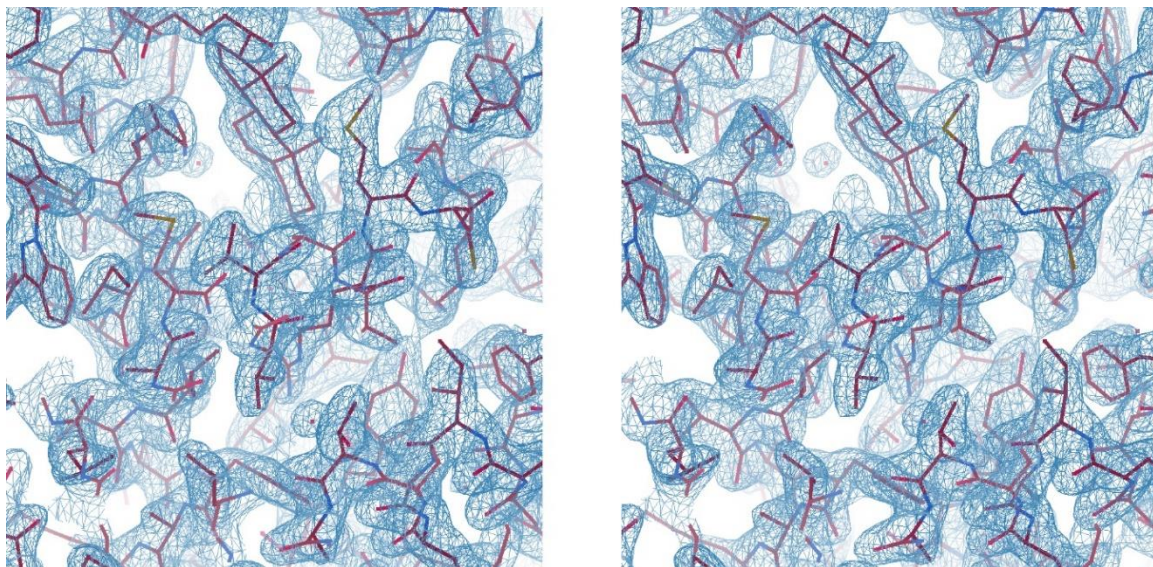
Fig. S18. Stereo image of a portion of the electron density map (2Fo-Fc) of RORγt in complex with 25-hydroxycholesterol and MRL-871 (6T4Y).
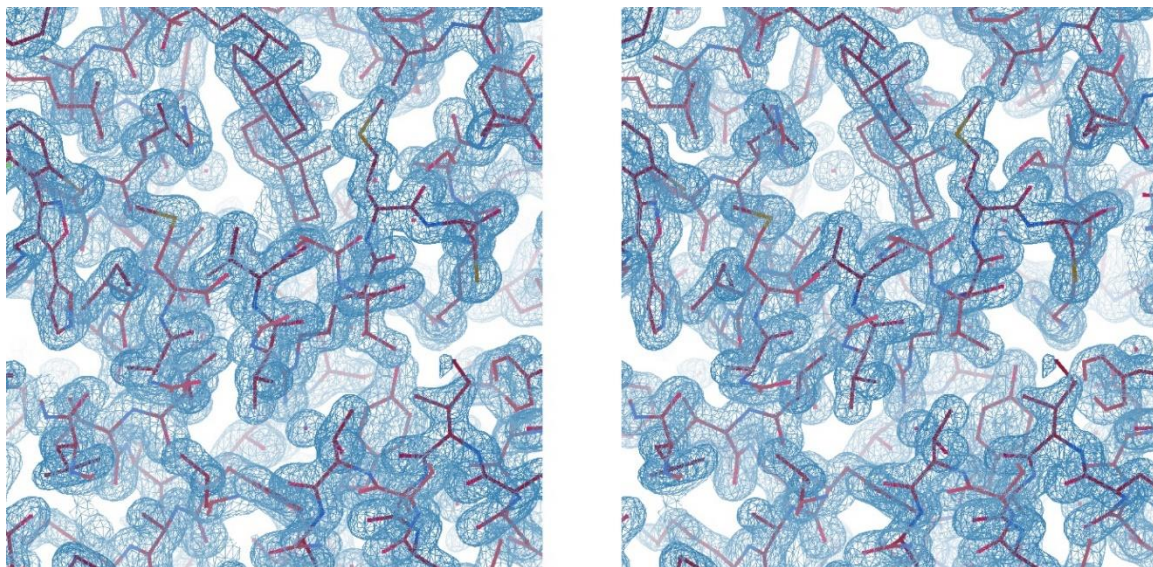
Fig. S19. Stereo image of a portion of the electron density map (2Fo-Fc) of RORγt in complex with 25-hydroxycholesterol and FM26 (6T4X).
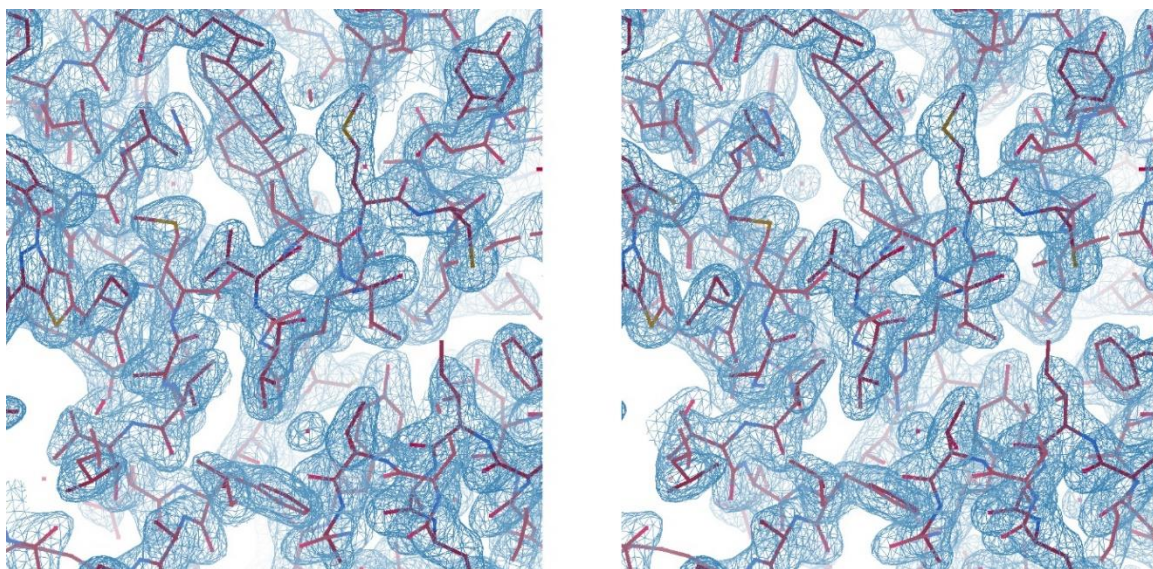
Fig. S20. Stereo image of a portion of the electron density map (2Fo-Fc) of RORγt in complex with 25-hydroxycholesterol and compound 13 (6T50).
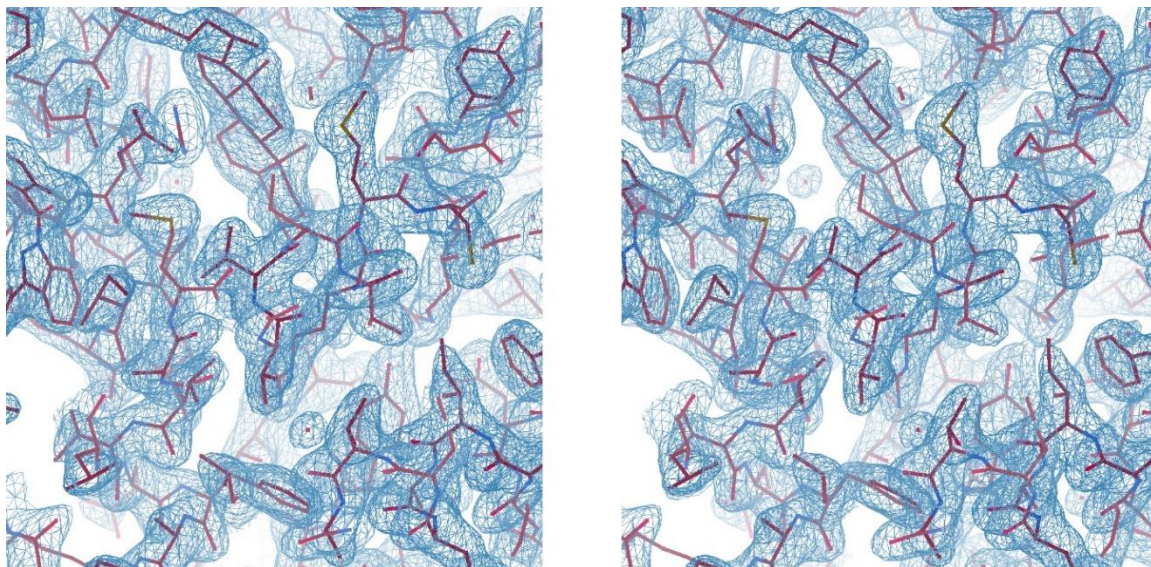
Fig. S21. Stereo image of a portion of the electron density map (2Fo-Fc) of RORγt in complex with desmosterol and MRL-871 (6T4K).
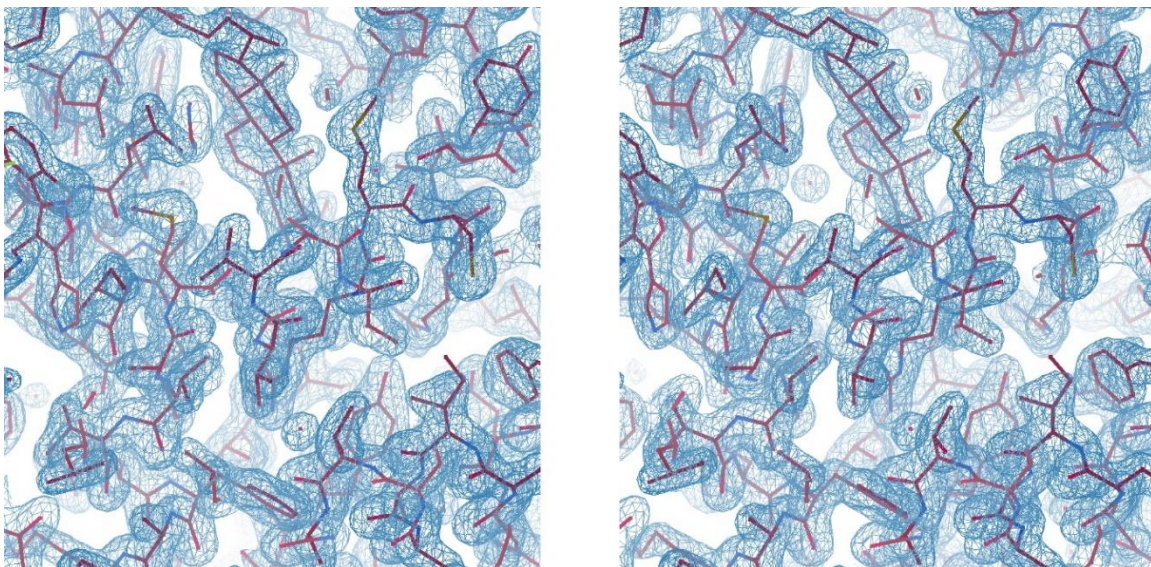
Fig. S22. Stereo image of a portion of the electron density map (2Fo-Fc) of RORγt in complex with desmosterol and FM26 (6T4J).
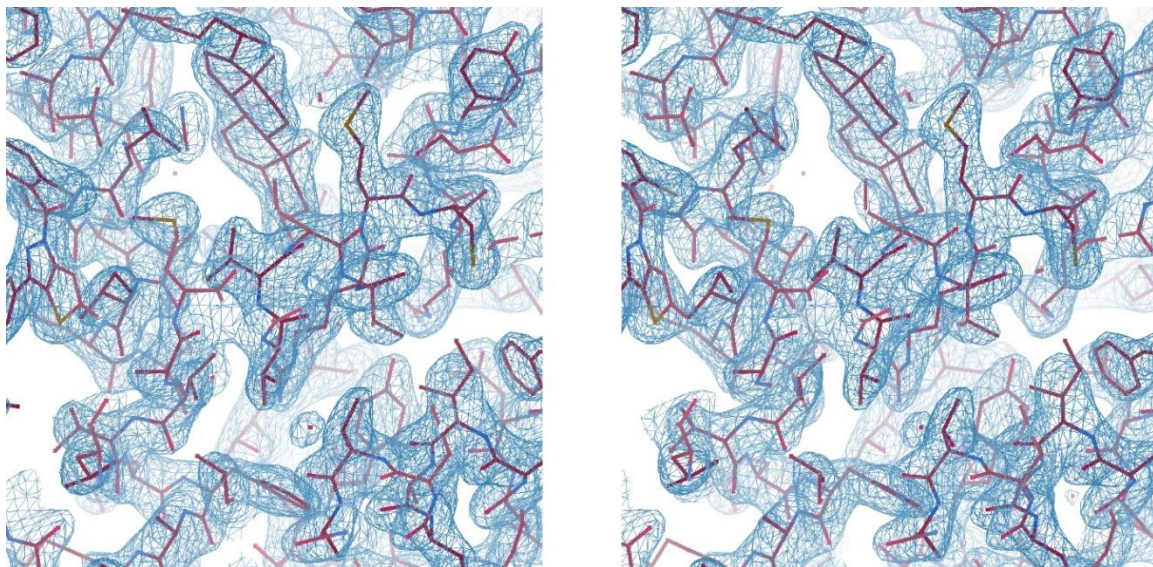
Fig. S23. Stereo image of a portion of the electron density map (2Fo-Fc) of RORγt in complex with desmosterol and compound 13 (6TLT).
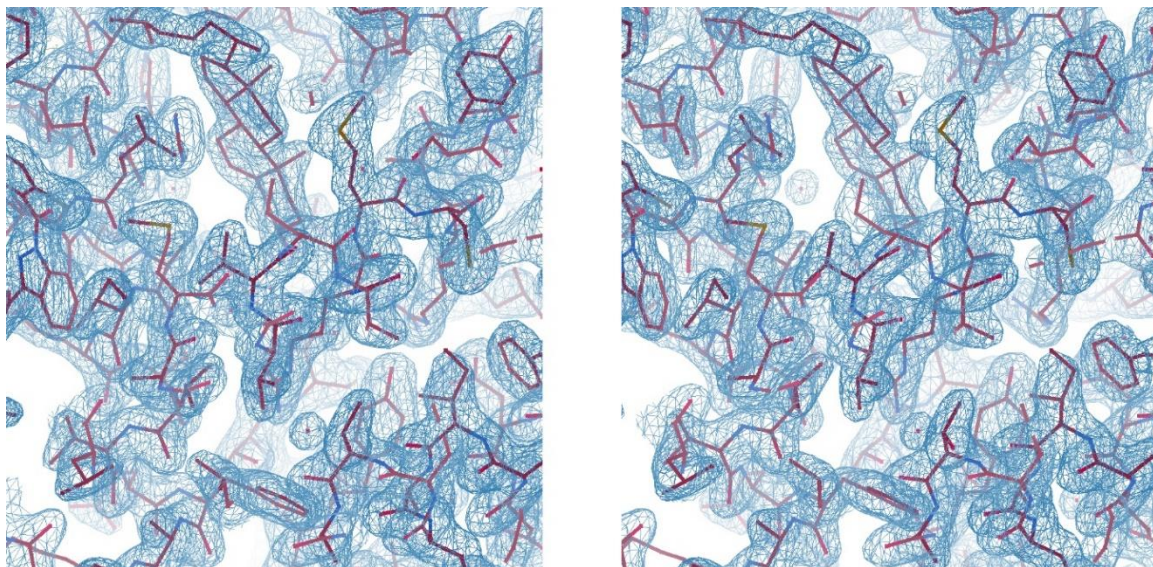
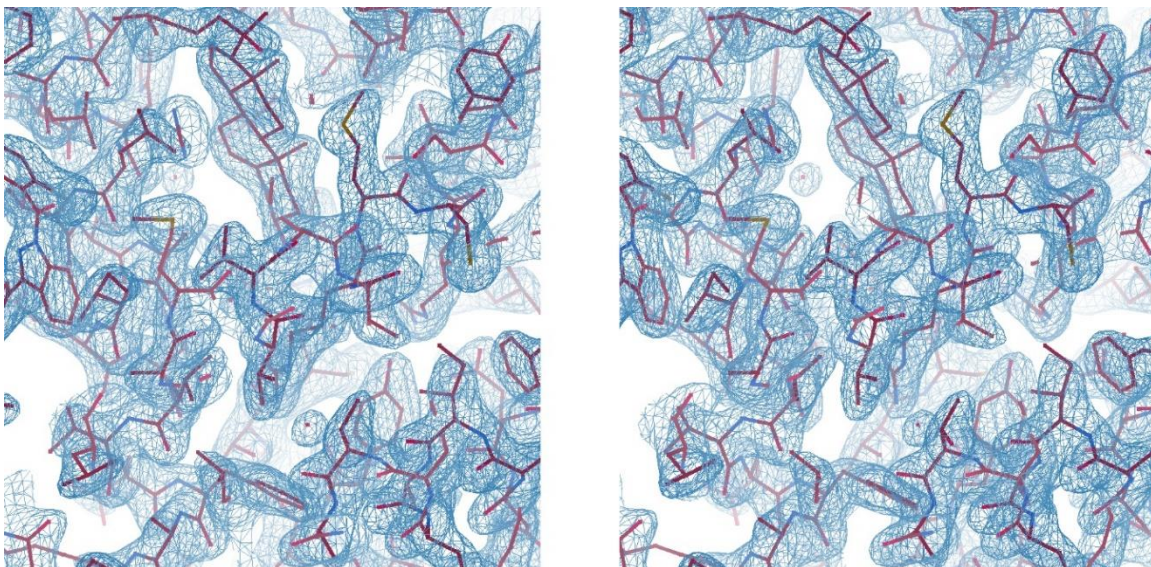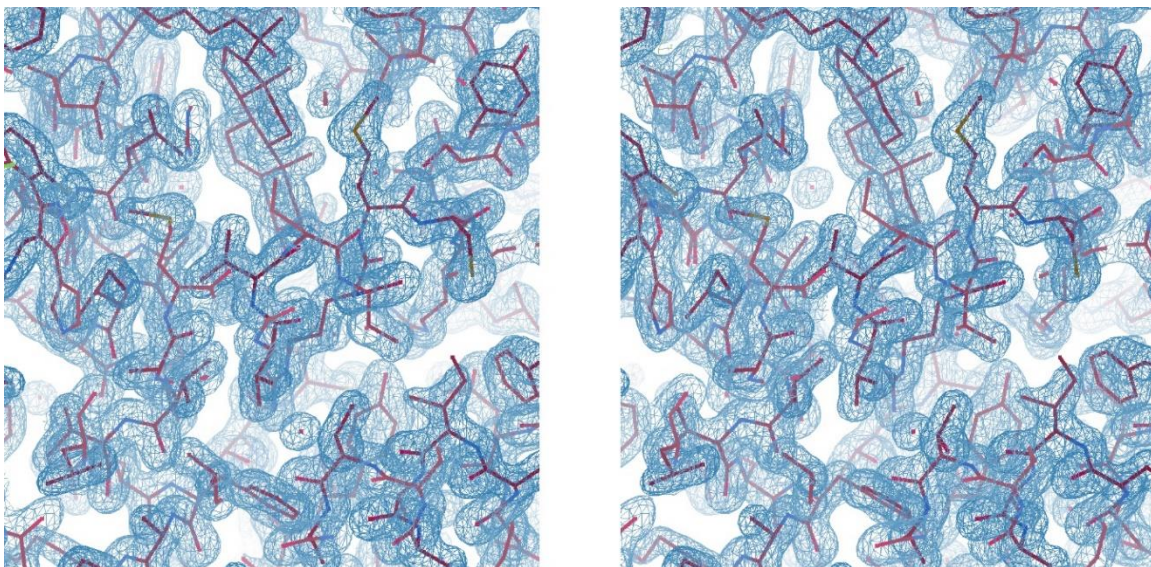**Fig. S24.** Stereo image of a portion of the electron density map (2Fo-Fc) of RORγt in complex with cholesterol and MRL-871 (6T4I).
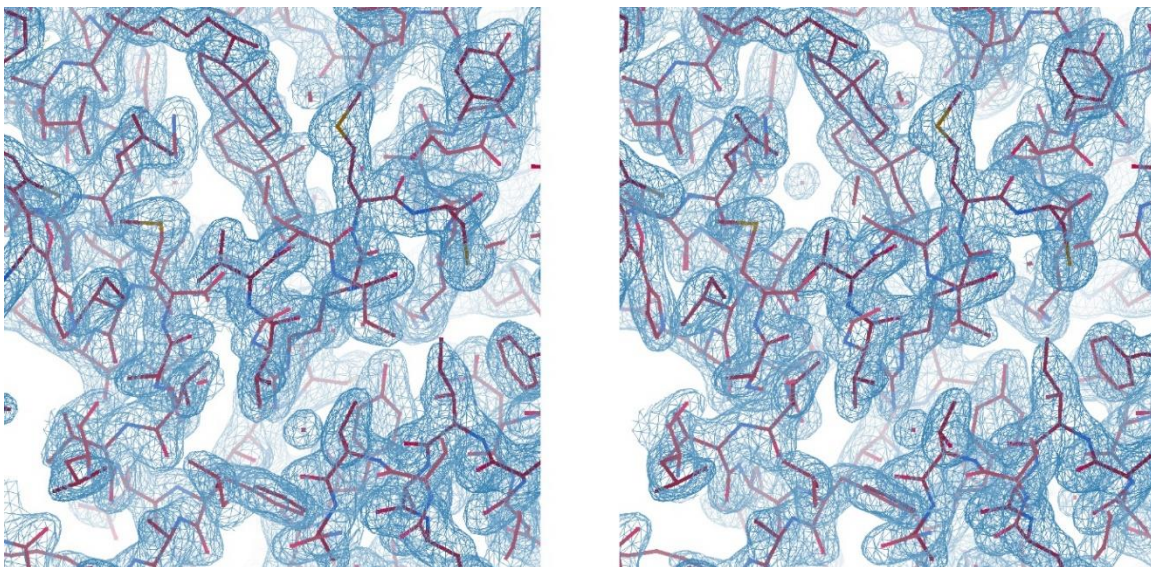
Fig. S25. Stereo image of a portion of the electron density map (2Fo-Fc) of RORγt in complex with cholesterol and FM26 (6T4G).
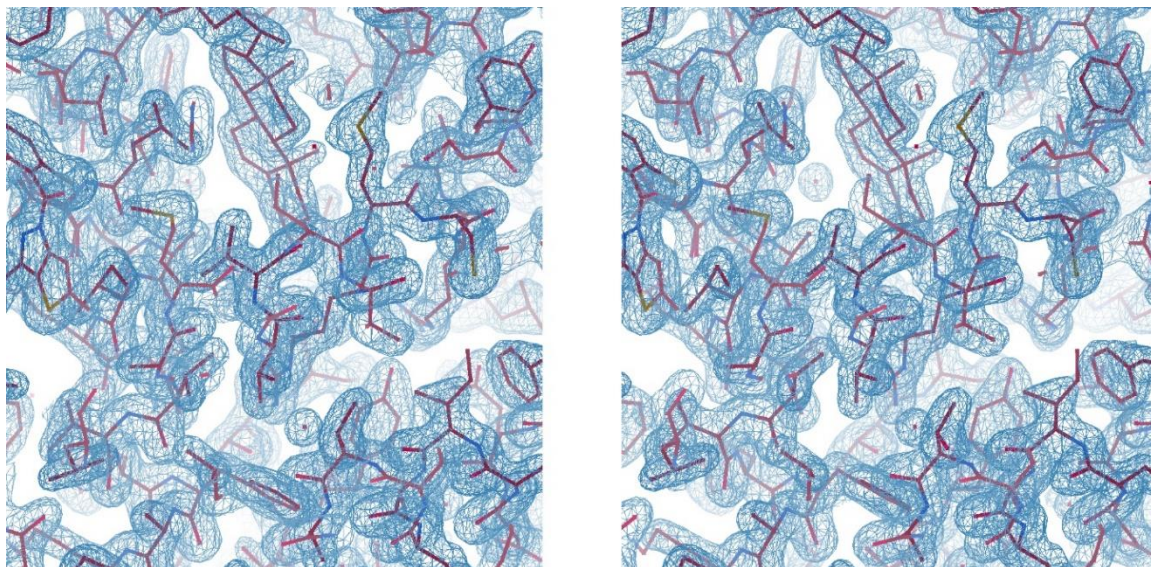
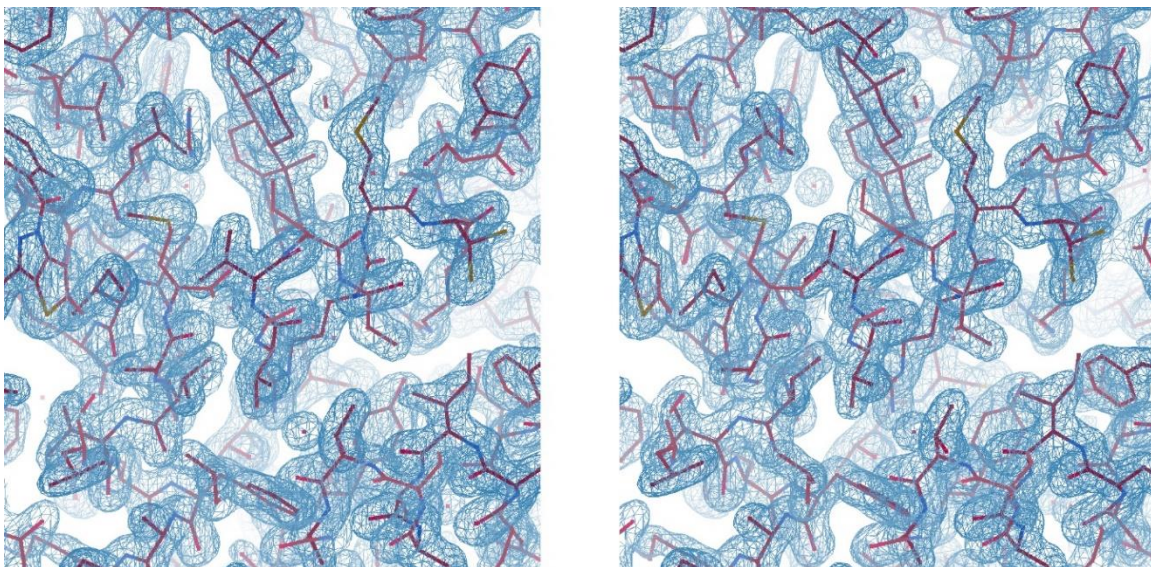**Fig. S26.** Stereo image of a portion of the electron density map (2Fo-Fc) of RORγt in complex with cholesterol and compound 13 (6TLQ).

Table S1. EC_{50} & IC_{50} values for all compounds, determined in TR-FRET coactivator assays.

	Compound	EC_{50}/IC_{50} (nM)
Orthosteric agonists	Cholesterol	416 ± 41
	Desmosterol	43.0 ± 7.3
	20α-hydroxycholesterol	24.0 ± 2.8
	25-hydroxycholesterol	Ambiguously
Orthosteric inverse agonist	Digoxin	15090 ± 1300
Allosteric inverse agonists	MRL-871	7.8 ± 0.5
	FM26	264 ± 23
	Compound 13	425 ± 61

Table S2. IC_{50} values observed in the competitive TR-FRET coactivator recruitment assay with fixed concentrations of orthosteric ligands cholesterol and titration of digoxin.

cholesterol concentration (μM)	Digoxin IC_{50} (nM)
0.00	7012 ± 588
0.25	33620 ± 1694
1.00	85400 ± 4276

Table S3. IC_{50} values observed in the competitive TR-FRET coactivator recruitment assay with fixed concentrations of orthosteric ligands 20α-hydroxycholesterol (20-OH), 25-hydroxycholesterol (25-OH), desmosterol (DSM) and cholesterol (CHL).

orthosteric ligand concentration (μM)	allosteric ligand				
	MRL-871 IC_{50} (nM)	FM26 IC_{50} (nM)	compound 13 IC_{50} (nM)		
0.00	10.1 ± 0.7	296 ± 34	514 ± 72	20-OH	orthosteric ligand
0.25	7.8 ± 0.3	55 ± 3	210 ± 19		
1.00	6.4 ± 0.2	79 ± 4	228 ± 24		
0.00	11.6 ± 0.6	249 ± 28	629 ± 173	25-OH	
0.25	7.5 ± 0.3	57 ± 2	155 ± 12		
1.00	5.2 ± 0.2	60 ± 4	131 ± 13		
0.00	10.2 ± 0.6	343 ± 35	466 ± 49	DSM	
0.25	7.5 ± 0.3	80 ± 4	130 ± 9		
1.00	5.0 ± 0.2	76 ± 4	148 ± 11		
0.00	12.7 ± 0.6	248 ± 18	547 ± 60	CHL	
0.25	9.4 ± 0.3	138 ± 6	300 ± 18		
1.00	7.8 ± 0.2	94 ± 3	269 ± 19		

Table S4. Overview of the crystallization conditions of RORγt. Abbreviations: 20α-hydroxycholesterol (20-OH), 25-hydroxycholesterol (25-OH), desmosterol (DSM), cholesterol (CHL) and compound 13 (CPD13).

Ligands	Crystallization Buffer	P:B* (nl)	Cryoprotection
20-OH + MRL-871	Empty**	-	1.6M AmSO4 + 0.1M Tris + 25 % glycerol (pH=8.5)
20-OH + FM26	Empty**	-	1.6M AmSO4 + 0.1M Tris + 25 % glycerol (pH=8.5)
20-OH + CPD13	Empty**	-	1.6M AmSO4 + 0.1M Tris + 25 % glycerol (pH=8.5)
25-OH + MRL-871	1.6M AmSO4 + 0.1M Tris (pH=8.5)	800 : 400	1.6M AmSO4 + 0.1M Tris + 25 % glycerol + 200 µM MRL-871 (pH=8.5)
25-OH + FM26	1.6M AmSO4 + 0.1M Tris (pH=8.5)	800 : 400	1.6M AmSO4 + 0.1M Tris + 25 % glycerol + 200 µM FM26 (pH=8.5)
25-OH + CPD13	0.2M MgCl2 + 6% PEG6000 + 0.1M Tris (pH=8.5)	800 : 400	0.2M MgCl2 + 6% PEG6000 + 0.1M Tris + 200µM CPD13 (pH=8.5)
DSM + MRL-871	0.2M MgCl2 + 6% PEG6000 + 0.1M Tris (pH=8.5)	900 : 300	0.2M MgCl2 + 6% PEG6000 + 0.1M Tris + 200µM MRL-871 (pH=8.5)
DSM + FM26	1.2M AmSO4 + 0.1M Tris (pH=8.5)	900 : 300	1.6M AmSO4 + 0.1M Tris + 25 % glycerol + 200 µM CPD13 (pH=8.5)
DSM + CPD13	1.6M AmSO4 + 0.1M Tris (pH=8.5)	800 : 400	1.6M AmSO4 + 0.1M Tris + 25 % glycerol + 200 µM FM26 (pH=8.5)
CHL + MRL-871	0.2M MgCl2 + 6% PEG6000 + 0.1M Tris (pH=8.5)	800 : 400	0.2M MgCl2 + 6% PEG6000 + 0.1M Tris + 200µM MRL-871 (pH=8.5)
CHL + FM26	1.2M AmSO4 + 0.1M Tris (pH=8.5)	800 : 400	1.6M AmSO4 + 0.1M Tris + 25 % glycerol + 200 µM FM26 (pH=8.5)
CHL + CPD13	1.6M AmSO4 + 0.1M Tris (pH=8.5)	800 : 400	1.6M AmSO4 + 0.1M Tris + 25 % glycerol + 200 µM CPD13 (pH=8.5)

* Crystallization drop composition, protein-ligand solution volume (P) : crystallization buffer volume (B)
** The protein ligand solution was evaporated using an empty buffer well

Table S5. Data collection and refinement statistics for RORγt in complex with both an orthosteric and an allosteric ligand. Abbreviations: 20α-hydroxycholesterol (20-OH), 25-hydroxycholesterol (25-OH) and compound 13 (CPD13).

RORγt in complex with:	20-OH + MRL-871	20-OH + FM26	20-OH + CPD13	25-OH + MRL-871
Data collection				
Space group	P 6_1 2 2	P 6_1 2 2	P 6_1 2 2	P 6_1 2 2
Cell dimensions				
a, b, c (Å)	108.52 108.52 105.94	108.50 108.50 99.29	108.32 108.32 99.33	108.64 108.64 107.67
α, β, γ (°)	90 90 120	90 90 120	90 90 120	90 90 120
Resolution (Å)	54.26-2.00 (2.07-2.00)	54.25-1.62 (1.68- 1.62)	54.16-1.71 (1.77-1.71)	93.97-1.95 (2.02-1.95)
$I/\sigma(I)$	10.13 (0.27)	23.04 (2.69)	31.00 (0.88)	28.39 (1.63)
Completeness (%)	97.86 (82.70)	99.60 (96.99)	99.86 (99.62)	99.97 (100.00)
Redundancy	27.6 (8.2)	137.1 (73.2)	37.4 (37.3)	38.9 (38.0)
$CC_{1/2}$	0.985 (0.551)	1.000 (0.977)	0.991 (0.219)	1.000 (0.741)
Refinement				
No. unique reflections	24921 (2070)	44254 (4235)	37646 (3706)	27179 (2667)
Rwork/Rfree	0.1923/0.2282	0.1478/0.1887	0.1596/0.2000	0.186/0.215
No. atoms (non-H)				
Protein	1978	2053	2016	2040
Ligand	66	73	69	66
Water	64	198	176	47
Average B-factors				
Protein	56.31	29.44	34.44	61.26
Ligand	46.63	26.11	31.76	50.67
Water	54.58	42.05	45.48	57.05
R.m.s. deviations				
Bond lengths (Å)	0.007	0.024	0.013	0.014
Bond angles (°)	0.820	1.850	1.820	1.710
Ramachandran				
Favored/allowed (%)	97.9/2.1	98.8/1.2	99.2/0.8	98.8/1.2
Outliers (%)	0.0	0.0	0.0	0.0
PDB ID	6T4U	6T4T	6T4W	6T4Y

Table S6. Data collection and refinement statistics for RORγt in complex with both an orthosteric and an allosteric ligand. Abbreviations: 25-hydroxycholesterol (25-OH), desmosterol (DSM) and compound 13 (CPD13).

RORγt in complex with:	25-OH + FM26	25-OH + CPD13	DSM + MRL-871	DSM + FM26
Data collection				
Space group	P 6_1 2 2	P 6_1 2 2	P 6_1 2 2	P 6_1 2 2
Cell dimensions				
a, b, c (Å)	108.88 108.88 98.54	108.33 108.33 108.51	108.32 108.32 108.52	108.91 108.91 98.48
α, β, γ (°)	90 90 120	90 90 120	90, 90, 120	90 90 120
Resolution (Å)	94.29-1.48 (1.53-1.48)	48.46-1.87 (1.94-1.87)	48.46-1.89 (1.95-1.89)	47.66-1.79 (1.85-1.79)
$I/\sigma(I)$	25.51 (1.87)	35.83 (1.61)	35.74 (1.67)	22.70 (1.82)
Completeness (%)	99.99 (100.00)	99.96 (100.00)	99.97 (99.97)	99.98 (100.00)
Redundancy	39.1 (39.5)	39.1 (39.4)	39.1 (40.4)	39.0 (40.1)
$CC_{1/2}$	1.000 (0.757)	1.000 (0.799)	1.000 (0.777)	1.000 (0.689)
Refinement				
No. unique reflections	30639 (2992)	31584 (3088)	30639 (2992)	32984 (3222)
Rwork/Rfree	0.1749/0.1852	0.1857/0.2108	0.1847/0.2055	0.175/0.197
No. atoms (non-H)				
Protein	2055	2040	2175	2046
Ligand	73	63	71	66
Water	255	241	71	186
Average B-factors				
Protein	28.79	55.11	59.92	36.46
Ligand	24.03	42.73	52.19	32.77
Water	42.38	53.75	56.28	48.35
R.m.s. deviations				
Bond lengths (Å)	0.017	0.015	0.014	0.009
Bond angles (°)	1.790	1.780	1.760	1.190
Ramachandran				
Favored/allowed (%)	99.2/0.8	98.0/2.0	98.4/1.6	98.8/1.2
Outliers (%)	0.0	0.0	0.0	0.0
PDB ID	6T4X	6T50	6T4K	6T4J

Table S7. Data collection and refinement statistics for RORγt in complex with both an orthosteric and an allosteric ligand. Abbreviations: desmosterol (DSM), cholesterol (CHL) and compound 13 (CPD13).

RORγt in complex with:	*DSM + CPD13*	*CHL + MRL-871*	*CHL + FM26*	*CHL + CPD13*
Data collection				
Space group	P 6₁ 2 2	P 6₁ 2 2	P 6₁ 2 2	P 6₁ 2 2
Cell dimensions				
a, b, c (Å)	108.73 108.73 104.73	107.96 107.96 107.42	108.51 108.51 105.04	108.86 108.86 98.64
α, β, γ (°)	90 90 120	90 90 120	90 90 120	90 90 120
Resolution (Å)	94.16-2.11 (2.16-2.10)	46.75-1.84 (1.91-1.84)	48.5-1.93 (2.00-1.93)	98.64-1.75 (1.78-1.75)
$I/\sigma(I)$	10.2 (0.5)	29.39 (1.15)	27.97 (1.81)	8.7 (0.5)
Completeness (%)	99.4 (92.0)	98.75 (92.59)	99.97 (99.96)	100.0 (99.8)
Redundancy	37.6 (38.8)	32.8 (13.7)	39.0 (40.0)	37.3 (35.7)
$CC_{1/2}$	0.999 (0.414)	1.000 (0.527)	1.000 (0.848)	0.998 (0.297)
Refinement				
No. unique reflections	21797 (1611)	32217 (2967)	28750 (2806)	35249 (1900)
Rwork/Rfree	0.196/0.235	0.191/0.214	0.178/0.213	0.178/0.212
No. atoms (non-H)				
Protein	2005	2053	2030	2042
Ligand	62	65	66	74
Water	17	113	105	181
Average B-factors				
Protein	66.01	52.32	52.30	35.61
Ligand	58.22	45.29	45.89	39.38
Water	56.45	54.27	53.92	46.39
R.m.s. deviations				
Bond lengths (Å)	0.016	0.015	0.016	0.017
Bond angles (°)	2.100	1.940	1.890	1.930
Ramachandran				
Favored/allowed (%)	98.4/1.2	99.2/0.8	99.2/0.8	98.8/1.2
Outliers (%)	0.4	0.0	0.0	0.0
PDB ID	6TLT	6T4I	6T4G	6TLQ

Movie S1 (separate file). Computational protein morph between the 6TLM and 6T50 structures using UCSF Chimera. This morph highlights the clamping motion of helix 4 of RORγt upon orthosteric ligand binding.